Light-Triggered Programming of Hydrogel Properties Using Sleeping Photoactive Polymer Nanoparticles

DOI:
10.1021/acs.chemmater.0c04400

Document Version
Accepted author manuscript

Light-Triggered Programming of Hydrogel Properties Using Sleeping Photoactive Polymer Nanoparticles

DOI:
10.1021/acs.chemmater.0c04400

Light-triggered programming of hydrogel properties using sleeping photoactive polymer nanoparticles

Amir H. Milani*, Jennifer M. Saunders, Nam T. Nguyen, Shanglin Wu and Brian R. Saunders*

Department of Materials, University of Manchester, MSS Tower, Manchester, M1 3BB, U.K.

Corresponding authors:

Amir H. Milani: amirhossein.milani@manchester.ac.uk

Brian R. Saunders: brian.saunders@manchester.ac.uk

ABSTRACT

A key characteristic of programmable hydrogels is that their physical and chemical properties can be changed post-synthetically. In order to achieve this, we used sub-50 nm photoacid/base generator nanoparticles, which could alter the charge density/polarity of a host macroscopic hydrogel (e.g. polyacrylamide). The photoacid generator nanoparticles (PAG), were composed of poly(methyl methacrylate-*co*-4,5-dimethoxy-2-nitrobenzyl methacrylate-*co*-1,6-hexanediol diacrylate) and exhibited pH-dependent swelling behavior when they were irradiated with UV light. Thus, using PAG nanoparticles enabled space-selective light-triggered swelling of host hydrogels by increasing the charge density at alkaline pH. Using photobase generator (PBG) nanoparticles, consisting of poly(methyl methacrylate-*co*-2-nitrobenzyl methyl 4-methacryloyloxy piperidine-1-carboxylate-*co*-1,6-hexanediol diacrylate), it was possible to space-selectively produce positive charge, at acidic pH, within the host hydrogel network. PBG nanoparticles added several functionalities to the host hydrogel, including reversible writing/erasing patterns as well as post-polymerization in desired sites. Including mixtures of PAG and PBG nanoparticles caused deswelling of the host hydrogel upon UV-irradiation. By increasing the mass fraction of PAG/PBG nanoparticles within the hydrogel, the deswelling effect was limited only to the top surface area, resulting in a monolayer actuator with a large bending angle. This study has successfully demonstrated the excellent potential of using

PAG/PBG nanoparticles to confer photo-responsive behaviors that transform non-responsive hydrogels into responsive hydrogels on demand. This system could be spatially tailored to provide a wide range of useful properties such as initiation sites for synthesis, writing/erasing and actuation.

1. Introduction

Hydrogels are composed of hydrophilic polymers which are physically or chemically crosslinked to form a 3D network that can hold large volumes of water. The unique properties of hydrogels such as their resemblance to the extra cellular matrix and their biocompatibility make them an excellent candidate for biomedical applications such as tissue engineering, drug delivery and soft robotics.[1-3] Programmable hydrogels with the ability of responding to external stimuli such as pH, temperature, electric field, ionic strength and light have been studied extensively.[4-5] Among all these stimuli, light has attracted more interest since it can be applied and tuned remotely in a spatiotemporal manner. Light-responsive hydrogels can respond in a variety of ways to irradiation by specific wavelengths. These responses include shape deformation, chemical modification, change in optical properties and alteration in charge density.[6-10] The latter plays a crucial role in swelling behaviors of hydrogels and also absorption/adsorption of charged species into/onto hydrogels via electrostatic interactions.[11-12]

There are numerous reports that propose preparation of photo-responsive hydrogels.[13-18] Javey and co-workers have developed a composite hydrogel which consisted of poly(*N*-isopropylacrylamide) and single-walled carbon nanotubes. The latter caused local heat generation, due to high absorbance of light in the near-IR region, which led to shrinkage of thermo-responsive hydrogel.[19] In a different approach Harada et al. used supramolecular chemistry based on α-cyclodextrin as the host component and azobenzene as a photo-responsive guest to prepare a light-triggered hydrogel actuator.[20] Other reported strategies include: utilizing photo-cleavable crosslinkers based on 2-nitrobenzyl derivatives[21] as well as incorporation of spiropyranes which alter their polarity by converting to zwitter ion species as a result of photoisomerism.[22] Despite the success in preparing photo-responsive hydrogels, most of these systems exhibit only one or a limited number of functionalities that are generated upon exposure to light.[22-23] These systems are often complicated to fabricate and multistep

synthesis are involved. Hence, applying such approaches to other frequently used hydrogels such as polyacrylamide may not be straightforward.[16, 24-25] A universal approach with capability of granting several functionalities is lacking for preparation of photo-induced multifunctional programmable hydrogels.

In this study light-triggered programming of hydrogel properties (LTPHP) was achieved by developing a binary system of photo-responsive nanoparticles which can work separately or together in order to alter charge density and polarity of non-ionic hydrogels upon irradiation by UV light. Using versatile 2-nitrobenzyl photo chemistry we prepare two types of sub-50 nm water-dispersible nanoparticles. Each system contains one type of photo-responsive group that converts into either acid or base when irradiated by UV light. Scheme 1 illustrates the chemical composition of PAG and PBG nanoparticles before and after photoreaction. The carboxylic acid groups that were generated upon UV-irradiation of PAG nanoparticles, caused them to swell at pH > pK_a (Scheme 1a). For the PBG nanoparticles the secondary amine groups were produced via photoreaction, however, unlike PAG nanoparticles no pH-dependent swelling behavior was observed (Scheme 1b).

PAG and PBG nanoparticles are easily embedded into non-ionic hydrogels (e.g. polyacrylamide) and confer pH-dependent properties in the local area of interest. Space-selective light-triggered generation of electrostatic charges, via deprotonation of acid or protonation of base groups, are shown to deliver multiple functionalities to hydrogels containing our new nanoparticles. These functionalities include space-selective swelling, absorption of small ions, adsorption of oppositely charged nanoparticles and actuation. Our general LTPHP approach introduces a novel and facile method to confer a variety of functionalities in non-ionic hydrogels which make them potentially useful in numerous applications in both material and biomaterial fields such as electronic devices and soft robotics.

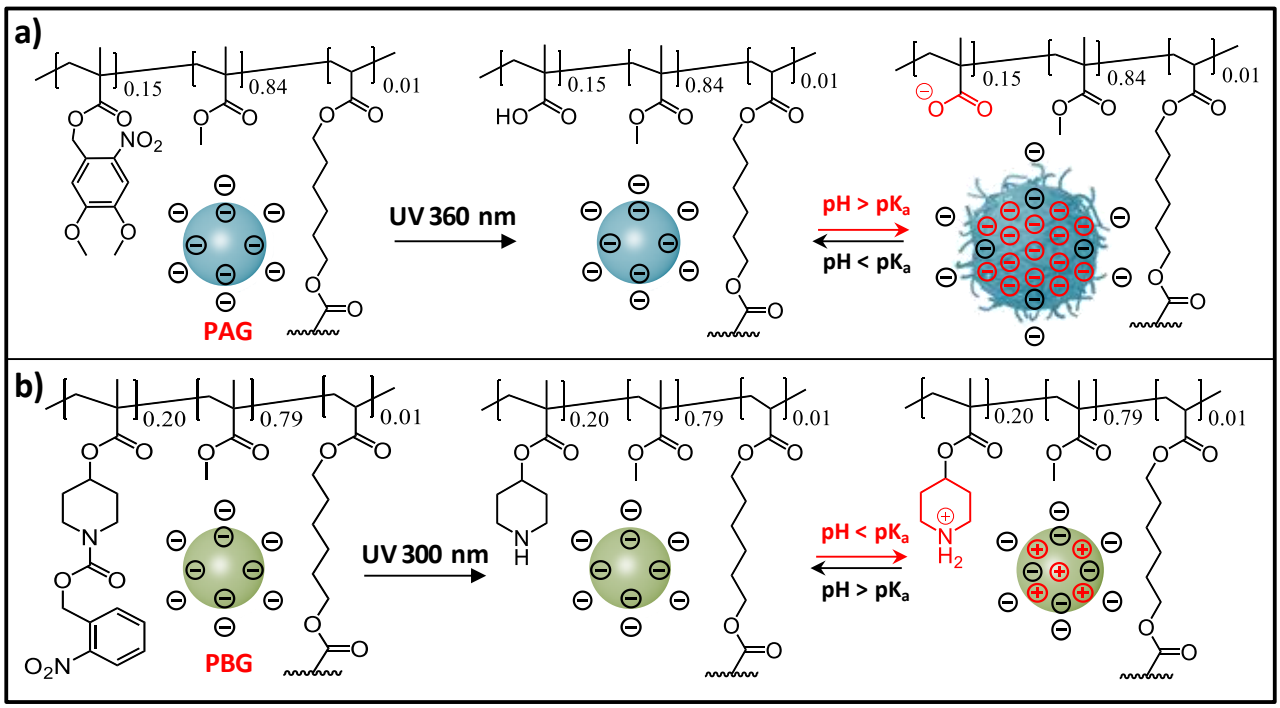

Scheme 1. (a) Chemical structure of photoacid generator nanoparticles (PAG). The PAG nanoparticles are stabilized by persulfate residues. UV-irradiation photo-generates carboxylic acids. Upon pH increase, at pH > pK_a, acid groups are deprotonated leading to an increase in charge density and swelling of nanoparticles. (b) Chemical structure of photobase generator nanoparticles (PBG). PBG nanoparticles are also stabilized via electrostatic repulsions between permanent negative charges. After UV-irradiation and reducing the pH positive charges are generated. PBG nanoparticles do not swell due to the presence of both negative and positive charges within the nanoparticles.

2. Experimental Section

2.1 Materials

Methyl methacrylate (MMA, 99%), sodium dodecyl sulfate (SDS, 98.5%), ammonium persulfate (APS, 98%), methacryloyl chloride (97.0%), *N*-*N*′-methylene bisacrylamide (MBA, ≥99.5%), acrylamide (AAm, ≥99.5%), triethylamine (TEA, 99%), 4,5-dimethoxy-2-nitrobenzyl methacrylate (DMNBM, 98%), 1,6-hexanediol diacrylate (HDODA, 80%), dichloromethane (DCM, 99.8%), *N,N,N′,N′*-tetramethyl ethylene diamine (TEMED, 99%), poly(ethylene glycol) diacrylate (PEGDA, M_n = 575 g/mol), poly(ethylene glycol) methacrylate (PEGMA, M_n = 500 g/mol), pyrrole (Py, 98%), 2-hydroxyethyl methacrylate (HEMA, 97%), iron(III) chloride (97%), sodium citrate dihydrate, (≥99%), sodium carbonate (>99.5%), $HAuCl_4 \cdot 3H_2O$ (>99.9%), Methylene Violet 3RAX (90%),

Orange II sodium salt (85%) and Brilliant Black BN (60%) were all purchased from Sigma-Aldrich. 2-Nitrophenyl methyl 4-methacryloyloxy piperidine-1-carboxylate (NPMPC) was obtained from Fujifilm Wako Chemicals. All chemicals were used as received unless otherwise stated. The water used in this work was deionized with a resistivity of 15 MΩ cm and was produced using a SLS Lab Pro PURA-Q2 water purifier.

2.2 Synthesis of 4,5-dimethoxy-2-nitrobenzyl methacrylate

4,5-Dimethoxy-2-nitrobenzyl methacrylate (DMNBM) was synthesized according to the literature[21] A solution of 4,5-dimethoxy-2-nitrobenzyl alcohol (2.40 g, 11 mmol) in dry DCM (160 mL) was added to a one-neck flask (500 mL) in an ice bath. TEA (1.73 g, 17 mmol) was added to the solution and allowed to stir for 5 min. Then methacryloyl chloride (1.68 g, 16 mmol) was added and the reaction mixture was left for 5 h to stir under an Ar atmosphere at room temperature. The reaction was stopped by washing with aqueous HCl solution (0.1 M, 100 mL ×2) and then brine. The DCM was removed by rotary-evaporation and the solid product was dissolved in acetone and precipitated in water. The precipitate was collected by filtration and dried in an oven at 50 °C overnight.

2.3 Synthesis of PAG and PBG nanoparticles

Both photoacid and photobase generator (PAG and PBG) nanoparticles were prepared via precipitation polymerization. The following describes a typical preparation for PAG nanoparticles. SDS (0.50 g, 2 mmol) was dissolved in a mixture of water (25.0 g) and acetone (20.0 g). The solution was added to a three-neck round bottom flask (250 mL) and purged with Ar for 15 min. An initiator solution of APS (0.0430 g, 0.19 mmol) in water (1.0 g) was then added and allowed to stir for 2 min. A monomer feed comprising DMNBM (0.080 g, 0.28 mmol), MMA (230.0 μL, 2 mmol), HDODA (2.0 μL, 0.08 mmol) dissolved in acetone (6.0 g) was then added to reaction vessel at a rate of 0.050 mL/min. The temperature of reaction was maintained at 70 ºC throughout polymerization and for a further 1 h after completion of the feed. The reaction was stopped by decreasing the temperature. The

product was dialyzed against water for 3 days and then purified using centrifugation at 14500 rpm for 30 min. For the synthesis of PBG nanoparticles the same method was used as described above. However, NPMPC (0.098 g, 0.28 mmol) was used in place of DMNBM. The physical and chemical characterization data for both PAG and PBG nanoparticles are tabulated in Table S1.

2.4 Hydrogels containing PAG nanoparticles

The hydrogel compositions are termed as PA/B-C(*x*) where A and B are, respectively, the hydrogel structural monomer and crosslinker. The parameter C identifies the type of embedded nanoparticles (i.e., PAG or PBG). The value of *x* is the concentration (wt %) of nanoparticles used. The chemical composition corresponding to each code is shown in Table S2.

Preparation of PAAm/MBA-PAG(4) hydrogel

AAm (0.0220 g, 0.31 mmol) and MBA (0.7 mg, 0.045 mmol) was dissolved in PAG dispersion (500 μL, 4.0 wt%) in a glass vial. The latter had an internal diameter of 2 cm. Then a solution of TEMED in water (11 μL, 0.24 M) was added. This was followed by addition of solution of APS in water (20 μL, 0.23 M). The mixed dispersion was purged with nitrogen and placed in an oven at 37 °C for 1 h. For the control gel water was used instead of the PAG dispersion. The rod-like sample was prepared by injecting the precursor dispersion (above) into a mold made from Al foil with an internal diameter of 1.25 cm. Al foil was also used as the photomask where required.

UV-irradiation of PAAm/MBA-PAG(4) hydrogel

The following describes the UV-irradiation method employed for the gels containing PAG nanoparticles. For UV-irradiation, samples were placed in the UV box (CL 1000 Ultraviolet Crosslinker) equipped with six 360 nm bulbs for 1 h intervals. The total intensity was 14 mW/cm^2. The experimental geometry employed during irradiation is depicted in Figure S1. Water was added to the top of each gel to prevent dehydration and maintained during irradiation. The volume of water added was 0.5 mL to 2 mL depending on the size of the gel. The as-made gel volumes varied from ~

0.2 mL to ~ 2 mL. The layer of water prevented the gels from becoming hot and did not cause additional gel swelling. After irradiation (or each irradiation interval) the sample was left in pH 9 carbonate-bicarbonate buffer (0.10 M) for 24 h and then left in water for another 24 h to reach maximum swelling. The same procedure was also used for the pH-dependent swelling studies.

Volume swelling ratio

A gravimetric method was used to measure the gel volume swelling ratio (Q_v). After 5 h of continuous exposure to UV light (360 nm), samples were placed in buffers with different pH values for 24 h and then soaked in water for another 24 h and then weighed. The following equation was used to calculate Q_v

$$Q_V = \rho_p \left(\frac{Q_{(m)}}{\rho_s} + \frac{1}{\rho_p} \right) - \frac{\rho_p}{\rho_s} \qquad (1)$$

where $Q_{(m)}$ is the mass swelling ratio. The parameters ρ_s and ρ_p are the densities of the solvent (water) and polymer, respectively. These values were taken as 1.0 and 1.3 g/mL.

Preparation of PEGMA/PEGDA-PAG(4) hydrogel

The gel was prepared and cured in a glass vial with internal diameter of 2.0 cm. PEGMA (0.067 g, 0.121 mmol) and PEGDA (0.0014 g, 0.002 mmol) were mixed with PAG dispersion (500 μL, 4.0 wt%.). To the latter mixture TEMED solution (11 μL, 0.24 M) and APS (20 μL, 0.23 M) were added and the dispersion mixed. Then the precursor was flushed with nitrogen and placed in an oven at 37 °C for 1 h. The sample was then placed in water for 24 h before UV treatment.

2.5 Hydrogels containing PBG nanoparticles

Preparation of PAAm/MBA-PBG(2) hydrogel film

To prepare PAAm/MBA-PBG(2) gel a precursor dispersion was prepared by dissolving AAm (0.0220 g, 0.31 mmol) and MBA (0.0007g, 0.045 mmol) in PBG dispersion (500 μL, 2.0 wt%).

TEMED solution (11 μL, 0.24 M) and APS (12 μL, 0.23 M) were then added in succession and the dispersion mixed. The precursor was injected into a mold made of a spacer sandwiched between two glass slides. The mold was then placed in oven at 50 °C for 10 min. The method used to prepare the PAAm/MBA-PBG(4) film was similar to PAAm/MBA-PBG(2). However, in that case a PBG dispersion (500 μL) with concentration of 4.0 wt% was used.

UV-irradiation of PAAm/MBA-PBG(2) hydrogel film

To prepare complex photomasks patterns were printed on a transparent A4 paper using a common black/white laser printer. Masked hydrogel films were placed in the UV box equipped with 300 nm UV bulbs for 1 h. The surface of exposed area was kept hydrated by wetting it with water occasionally as required as described above. For the gels containing PBG nanoparticles six 300 nm bulbs were used for UV irradiation.

2.6 Physical Measurements

Dynamic light scattering (DLS) data and zeta potential data were measured using a Malvern Zetasizer NanoZS instrument fitted with a 20 mW HeNe laser. The angle of detection was set at 173°. ^{1}H NMR spectra were obtained using a B400 Bruker Avance III 400 MHz spectrometer. SEM images were captured using a FEG TESCAN MIRA3 SEM equipped with backscattering (BS) and EDX detectors. EDX images were obtained by scanning the area of interest for 15 min. Hydrogel samples were first freeze-dried and then coated with carbon before SEM imaging. Potentiometric titration was performed using a Mettler Toledo titration instrument. UV-visible spectra were measured using a VWR UV-6300PC double beam spectrophotometer. TEM images were obtained using a FEI Tecnai 12 BioTwin instrument. TEM samples were deposited on a holey carbon-coated copper grid and were stained using uranyl acetate solution (0.50 wt%). Image-J software was used to determine the number-average diameter of the nanoparticles. Dynamic rheology data were obtained using a TA Instruments AR G2 rheometer. A 20 mm diameter plate geometry was used and the gap was 2000 μm. Electrical

conductivity measurements were performed using an in-house built four-probe system. The electrical conductivity of each half of hydrogel film was measured using four-probe technique and the following equation[26]:

$$\sigma = \frac{I}{2\pi SV} \qquad (2)$$

where σ is conductivity of bulk material, V and I are voltage and current respectively and S is distance between each probe. Since the value of I and S were fixed in this test, by measuring the voltage conductivity can be measured.

Further experimental details for fabrication and post-synthesis modification of hydrogels containing PAG/PBG nanoparticles are available in the Supporting Information.

3. Results and Discussion

3.1 Synthesis and characterization of photoacid/base generator nanoparticles

We synthesized sub-50 nm photoacid generator nanoparticles (PAG) consisting of poly(methyl methacrylate-*co*-4,5-dimethoxy-2-nitrobenzyl methacrylate-*co*-1,6-hexanediol diacrylate) and photobase generator nanoparticles (PBG) composed of poly(methyl methacrylate-*co*-2-nitrobenzyl methyl 4-methacryloyloxy piperidine-1-carboxylate-*co*-1,6-hexanediol diacrylate) using precipitation polymerization. The PAG and PBG nanoparticles were stabilized by electrostatic repulsion from an anionic surfactant (SDS) and permanent negative charges from the persulfate initiator residue. Dialysis and centrifugation was used to remove SDS after synthesis and consequently the major source of negative charge for both the PAG and PBG particles is the persulfate residues. 1,6-Hexanediol diacrylate was included as a crosslinker in both systems.

The photo-reactive monomer incorporated in PAG was synthesized according to literature[21] and the ^{1}H NMR analysis confirmed a high conversation of 99 % (Figure S2). The monomer ratios for each system were also measured by ^{1}H NMR spectroscopy (Figure S3 and S4) and these confirmed the

presence of 15 and 20 mol% of photo-cleavable nitrobenzene groups in PAG and PBG nanoparticles respectively. For the PAG nanoparticles the photo-reaction product is a carboxylic acid[27] which generates negative charge upon deprotonation (Scheme 1a). The PAG nanoparticles show a maximum absorbance at 360 nm due to presence of 4,5-dimethoxy-2-nitrobenzyl group[28] (Figure S5). After UV-irradiation of the PAG nanoparticles with 360 nm UV light, they acted as pH-responsive nanogels and swelled at pH > pK_a[29]. Potentiometric titration data indicated an apparent pK_a value of 7.4 and RCOOH content of 10 wt% after UV-irradiation of dilute PAG dispersion (0.2 wt%) for 1 hour (Figure S6). The pH dependent swelling behavior of PAG nanoparticles was investigated by dynamic light scattering (DLS). The DLS data showed a z-average (d_z) value of 36 nm for collapsed PAG nanoparticles at pH 4 before UV-irradiation (Figure 1a).

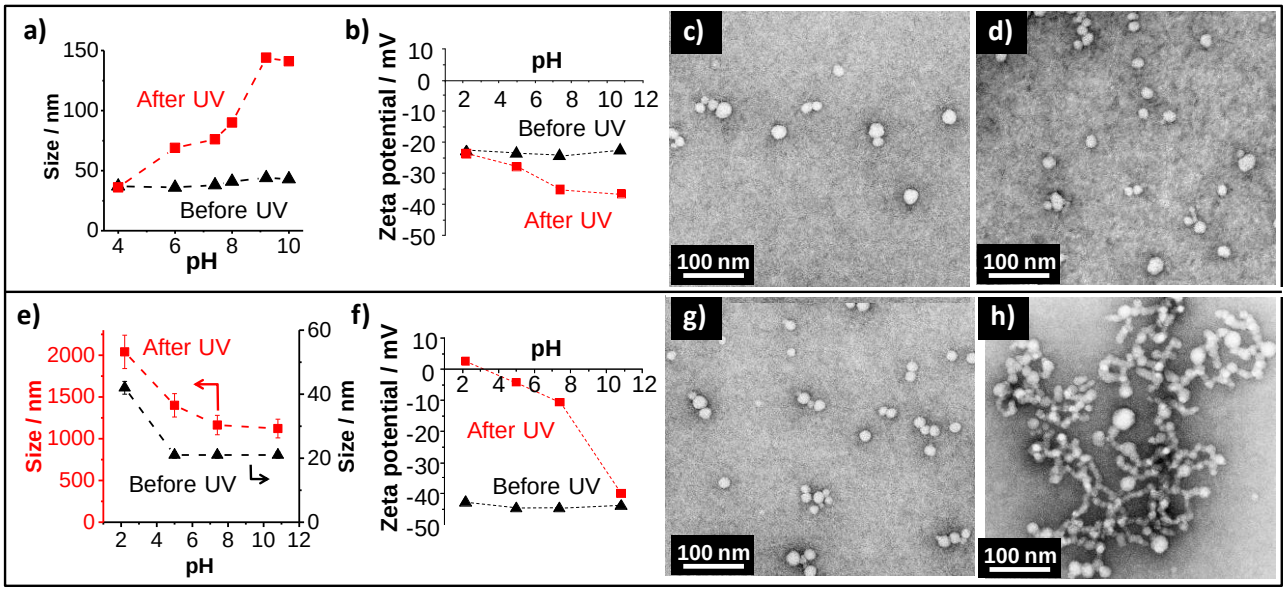

Figure 1. (a) DLS measurements for PAG nanoparticles before and after UV-irradiation at different pH values. The PAG nanoparticles showed pH-dependent swelling behavior after UV-irradiation. (b) Zeta potential for PAG nanoparticles measured at different pH values before and after UV-irradiation. (c) and (d) TEM images of PAG nanoparticles before and after UV-irradiation respectively. (e) DLS data showing d_z vs pH for PBG nanoparticles before and after UV. (f) Zeta potential values against pH for PBG nanoparticles before and after UV. TEM images are shown for the PBG nanoparticles (g) before and (h) after UV-irradiation. All of the dispersions used to deposit the samples for TEM observation had a pH of about 5.0.

The PAG nanoparticle d_z value did not change significantly by increasing the pH. After UV-irradiation the d_z value at pH 4 was identical to that of before UV as the nanoparticles remained collapsed and did not aggregate. Importantly, the d_z increased when the pH was raised and reached a value of 147 nm at pH 9.2 (Figure 1a). The volume swelling ratio (Q) vs pH also changed significantly for PAG nanoparticles after UV-irradiation and it increased to the highest value (Q = 64) at pH 9.2 (Figure S7). The Q value is comparable to that of other polyacid microgel/nanogel nanoparticles reported in the literature.[30-31] Zeta potential measurements for PAG nanoparticles were performed at different pH values before and after UV-irradiation. The zeta potential shifted towards larger negative values for the UV-irradiated sample but for the parent (non-irradiated) sample the zeta potential was independent of pH value and did not change substantially (Figure 1b). Both pH-dependent swelling of PAG nanoparticles and zeta-potential data confirmed generation of negative charges at high pH when PAG nanoparticles were subjected to UV light. Transmission electron microscopy (TEM) was

employed to observe the morphology of nanoparticles and determine collapsed size as well. TEM images of PAG nanoparticles before and after UV exposure are shown in Figure 1c and 1d respectively. The number-average diameters (d_{TEM}) before and after UV at pH 4 were measured as 21$\pm$ 6 nm and 23 $\pm$ 7 nm (Figure S8) which were not significantly different to the respective d_z values.

The PBG nanoparticles were expected to produce secondary amine groups as the product of photochemical reaction (Scheme 1b).[32] The amine group was positively charged when protonated. The UV-visible spectrum of PBG nanoparticles showed a maximum absorption at 265 nm (Figure S9) because of 2-nitrobenzyl groups [28]. The as-made d_z value of PBG nanoparticles (pH 5) was 21 nm (Figure 1e). An increase in d_z at pH 2 is apparent for the non-irradiated PBG particles which is likely due to partial aggregation. A higher pH of ~ 5 was used to prepare the gels. We used a 300 nm UV lamp to irradiate these nanoparticles. The UV-irradiation of PBG nanoparticles caused immediate aggregation due to attraction between photo-generated positive charges and pre-existing negative charges on the nanoparticles. A large increase in d_z was observed from the DLS measurement for UV-irradiated PBG (see Figure 1e). The zeta potential values moved towards positive values for the UV-irradiated PBG nanoparticles by lowering the pH, which confirmed photo-generation of the positive charges on the nanoparticles (Figure 1f). A similar pH dependent shift in the zeta potential value has been reported for cationic microgel nanoparticles. [33-34] For the irradiated PBG nanoparticles the d_z values were all very large (> 1000 nm) indicating that the initial UV-triggered aggregation persisted at all the pH values studied. Any pH-triggered inter-particle repulsive electrostatic interactions were insufficient to completely break up the initial aggregates. Figure 1g and 1h illustrates TEM images of PBG nanoparticles before and after UV-irradiation respectively. Formation of large aggregation was also observed in UV-irradiated sample which confirmed that photo-triggered aggregation occurred. The d_{TEM} value of non-irradiated PBG nanoparticles was calculated as 18 $\pm$ 4 nm which was close to d_z value and also confirmed absence of aggregation prior to irradiation (Figure S10).

3.2 Photo triggered swelling of hydrogels containing photoacid/base generator nanoparticles

Since PAG nanoparticles showed a high swelling ratio we utilized them to control swelling of two different types of macroscopic hydrogels (i.e. based on acrylamide or PEG). These gels are being used widely in bio-related applications such as drug delivery, cell encapsulation and biosensors.[35-39]

Figure 2 shows hydrogels composed of poly(acrylamide-*co*-methylene-bis-acrylamide) / PAG nanoparticles, called PAAm/MBA-PAG(4). The PAG nanoparticles concentration was 4.0 wt%. These hydrogels became photo-responsive due to PAG nanoparticles. The morphology of freeze-dried PAAm/MBA-PAG(4) hydrogel film was studied by SEM and representative images are shown in Figure S11. In Figure 2a the as-made hydrogel is shown which was subjected to 360 nm UV light for different amounts of time. After each UV-irradiation the hydrogels were placed in pH 9 phosphate buffer (0.1 M) for 24 h and water for another 24 h. After five sequences of UV-irradiation the diameter of hydrogel disc almost doubled compared to that of the non-irradiated gel. The photo-triggered swelling of macroscopic hydrogels used in this study can be related to presence of PAG nanoparticles which upon UV-irradiation generate carboxylic acid groups and confer the parent hydrogel with a pH-responsive characteristic.

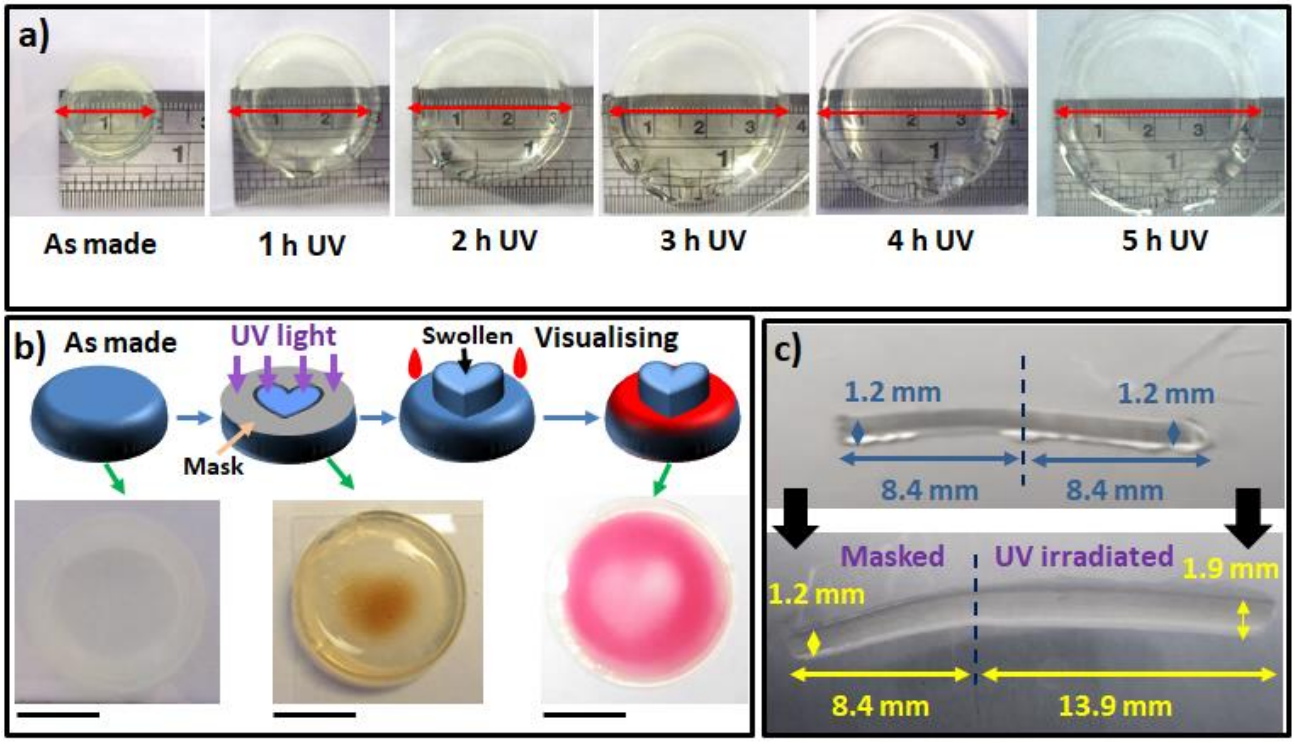

Figure 2. (a) Light-triggered swelling of PAAm/MBA-PAG(4) hydrogel with altering time of UV exposure. (b) Patterned light-swelling of PAAm/MBA-PAG(4). A photomask with a heart-shape cut out of it was used. After UV-irradiation and local swelling of the heart-shaped region of the hydrogel, cyanidin chloride dye was added to visualize the vertical swelling effect. The scale bar indicates 1 cm. (c) UV-irradiation on one half of rod-like PAAm/MBA-PAG(4). Both longitudinal and lateral swelling were observed on the UV-irradiated part.

Gel volume swelling ratio (Q_v) measurements were also conducted at a range of pH values for PAAm/MBA-PAG(4) and PAAm/MBA as control (Figure S12). The PAAm/MBA-PAG(4) hydrogel exhibited pH-dependent swelling and the Q_v value increased from 40 at pH 4 to 100 at pH 9. In contrast the PAAm/MBA control Q_v did not change significantly. Other techniques for photo-triggered swelling of hydrogels are mainly based on photo-cleavage of crosslinks or change in configurational isomerism of photo-sensitive component.[40-41] The advantage of our approach is that it does not require synthetic pre-functionalization of the hydrogel. Rather, the hydrogel is prepared in the usual way in the presence of added nanoparticles which then become encapsulated. The rate of gel switching should depend on the rate of photo-cleavage and also the rate of gel swelling. In principle, the rate of photo-cleavage could be increased by increasing the UV-irradiation intensity and increasing the rate of removal of the reaction byproducts. The rate of gel swelling will be limited

by diffusion of water through the nanometer-sized hydrogel mesh. This could be increased using a lower polymer concentration and/or a lower concentration of crosslinking monomer.

Spatially-controlled swelling of hydrogels can be used, to control cell interactions with hydrogel surfaces.[42] The ability of spatially-selective swelling of hydrogels was also demonstrated. For this purpose, a heart-shaped stencil was used on top of a disc like hydrogel sample. Figure 2b shows that after UV-irradiation, the heart-shaped region of the gel area that was UV-irradiated swelled more than the photo-masked area. The swelling was visualized by addition of a dye solution (cyanidin chloride) on top of heart-shaped region which was more elevated (due to swelling) than the masked region. The dye solution flowed from the heart-shaped region and collected due to gravity on previously masked parts of the gel that had not swollen. The dye did not have time to diffuse into the irradiated or masked regions of the gel during the experiment. To further demonstrate the ability of spatially-controlled photo triggered swelling using different sample geometries, a rod-like sample was prepared and only one half of the rod UV-irradiated (see Figure 2c). After leaving the sample in alkaline buffer followed by soaking in water similar to Figure 2a, the UV-irradiated area expanded both crosswise and lengthwise. The Q_v values were 16 and 62 for the masked half and UV-irradiated half respectively. This indicates a 4-fold increase in volume for the UV-irradiated half compared to the control half.

In order to demonstrate the generality of our technique, we also prepared poly(PEGMA-*co*-PEGDMA) / PAG hydrogel, termed PEGMA/PEGDA-PAG(4). A similar photo-triggered swelling effect to that of acrylamide based hydrogel was observed (see Figure S13). These data demonstrate the generality of our LTPHP method. By utilizing dormant PAG nanoparticles we were able to successfully produce encapsulated polyelectrolyte nanoparticles within non-ionic hydrogels spatiotemporally and transform them to a pH-responsive system.

3.3 Complex pattern formation and erasing on hydrogels

We prepared the PAAm hydrogels using APS as the initiator which provided negative charges from $–OSO_3^-$ groups within the hydrogel network. Although the PBG nanoparticles did not swell when

photo-irradiated, they showed a pronounced change in their charge (Figure 1f). Hence, the ability to switch the charge polarity from negative (due to local to $–OSO_3^-$ groups in PAAm/MBA) to positive (due to secondary amine groups in irradiated PBG) for a PAAm/PBD hydrogel was investigated. We found that by UV-irradiation of PAAm/MBA-PBG(2) hydrogel (Figure 3a(i)) using a patterned photomask, it was possible to switch the net electrostatic charge of the UV-irradiated area from negative to positive. In Figure 3a(ii) the PAAm/MBA-PBG(2) hydrogel film, which was covered with QR code patterned photomask, was UV-irradiated and left in acidic solution containing *anionic* Brilliant Black BN dye. After washing with water the pattern appeared because the negatively charged dye molecules absorbed to the photo-triggered positively charged sites (Figure 3a(iii)).

However, the positive charge of amine groups generated by UV light is removed at pH $\geq$ 9. Thus, by altering the pH it was possible to control absorption/desorption of the dye and consequently achieve reversible writing/erasing on the hydrogel (Figure 3a(iv)). A unique characteristic of this technique is the capability of writing a hidden message and to have it appear on demand. Figures 3b and 3c show that the QR code was printed with a high resolution and was readable by a smartphone. Several works have been published that proposed different techniques for writing on hydrogels including using supramolecular complex, flavylium salts and polyoxometalate ions.[43-45] Comparing our LTPHP approach to those approaches, no chemical modification is required to the hydrogel. A reviewer suggested that experiments be conducted to test the ability to repeatedly generate the QR code over multiple cycles pointing out that some light-responsive systems undergo photodegradation with time. We agree that such experiments are important for future application of this technology. Unfortunately, we were not able to conduct these experiments due to resource limitations and must defer them to future work.

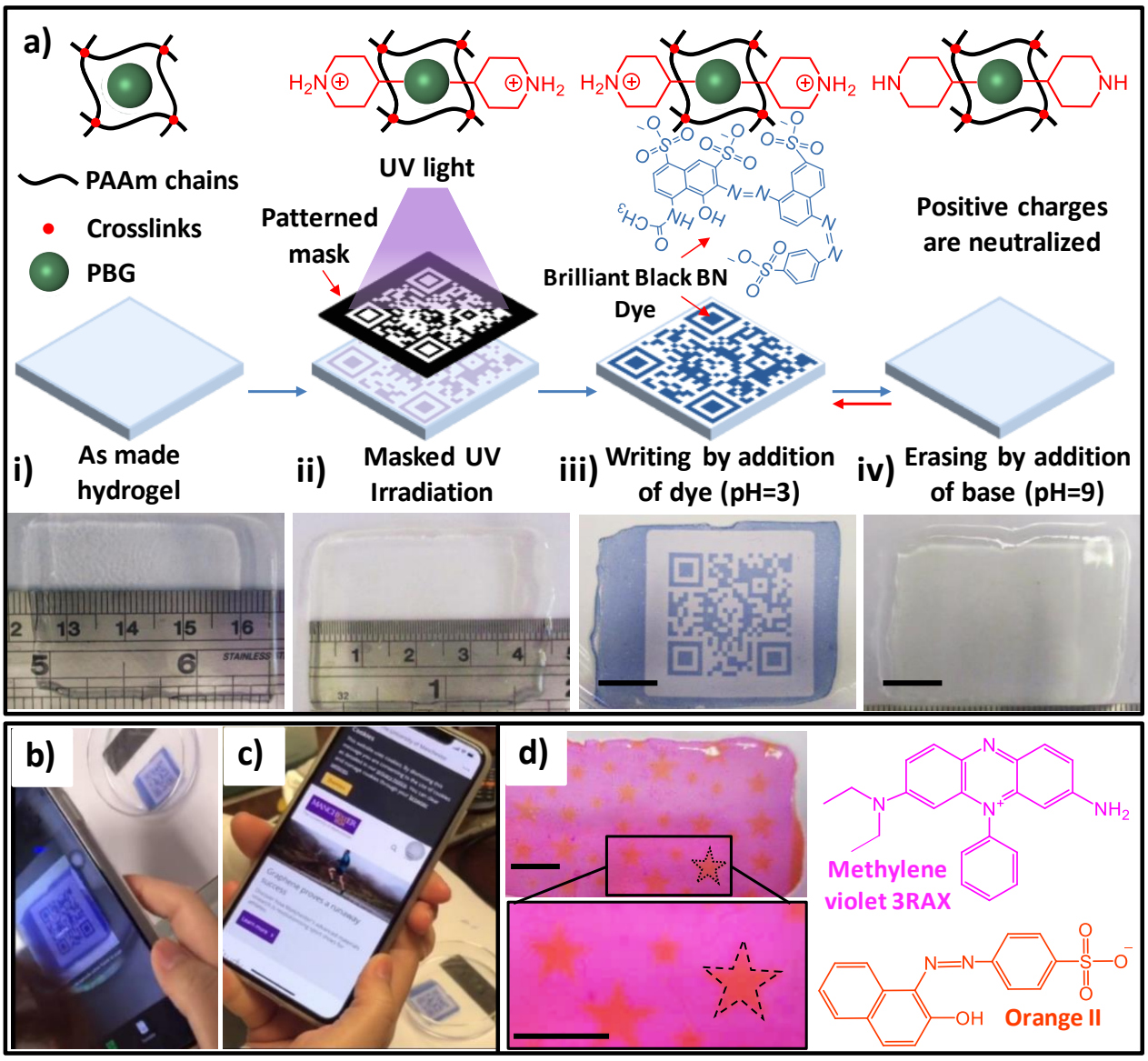

Figure 3. Writing/erasing on PAAm/MBA-PBG(2) hydrogel a(i)-a(iv). A sample was masked (QR code) and UV-irradiated for 1 h, then pH decreased to 2 to increase the number of positive charges. A negatively charged dye (Brilliant Black BN) was added and absorbed in the UV-irradiated areas which resulted in the appearance of a QR code. By washing in pH 9 buffer the negatively charged dye detached from uncharged –R_2NH groups and the pattern disappeared. The scale bars in 3a(iii) and 3a(iv) are 1 cm. (b) and (c) show scanning and reading of the QR code by a smartphone. (d) shows dichromatic drawing on PAAm/MBA-PBG(2) as well as chemical structure of dyes used. The scale bars are 5 mm.

We have also studied the effect of pH and irradiation time on Brilliant Black BN dye as well as the reversibility. It was observed that extending UV-irradiation time as well as decreasing pH, both increased absorption of dye due to generation of a larger number of positive charges. Figure S14a-d show that the main dye absorption at λ_{max} (580 nm) increased 4 times at pH 2.2 when UV-irradiation

time was doubled from 15 to 30 min. Similarly, absorption at λ_{max} was raised by a factor of 5 by decreasing the pH from 9 to 2 for the sample UV-irradiated for 30 min. The area of sample, which was masked as a control during UV-irradiation, did not show significant pH-dependent dye absorption (Figure S14d). Good reversibility in absorption/desorption of dye was demonstrated by conducting UV-visible spectroscopy measurements at two extreme pHs (1 and 13) for 3 cycles (see Figure S14e).

A unique feature of our LTPHP approach is the ability of drawing two-color patterns on hydrogels. We achieved this by introducing both negative (Orange II) and positive (Methylene violet 3Rax) dyes to the UV-irradiated PAAm/MBA-PBG(2) hydrogel (See Figure 3d). The negatively charged dye was selectively absorbed into UV-irradiated area while the positively charged dye stained the masked area which possessed negative charge due to the $–OSO_3^-$ groups. This proves the ability of the LTPHP approach to direct absorption of charged molecules selectively into specific locations of a gel.

3.4 Spatially-selective adsorption of charged nanoparticles onto the hydrogel

Selective adsorption of gold nanoparticles onto hydrogels is potentially useful for soft electronics[46] and patterned cell adhesion.[47] Negatively charged gold nanoparticles (GNP) were adsorbed onto the surface of PAAm/MBA-PBG(2) hydrogel at positively charged sites that had undergone spatially controlled photo-irradiation. The GNPs used in this study had a diameter of 15 nm (see Figure S15) and possessed negative charge due to presence of citrate group.[48] Figures 4a-4c shows PAAm/MBA-PBG(2) hydrogel film before/after UV-irradiation and after GNP deposition. After UV-irradiation the color of the irradiated area became yellow (see Figure 4b) due to formation of 2-nitrosobenzaldehyde as a by-product of photochemical reaction.[27] However, after leaving the sample in GNP dispersion, the target area became pink (Figure 4c) which is a signature of adsorption of GNPs.

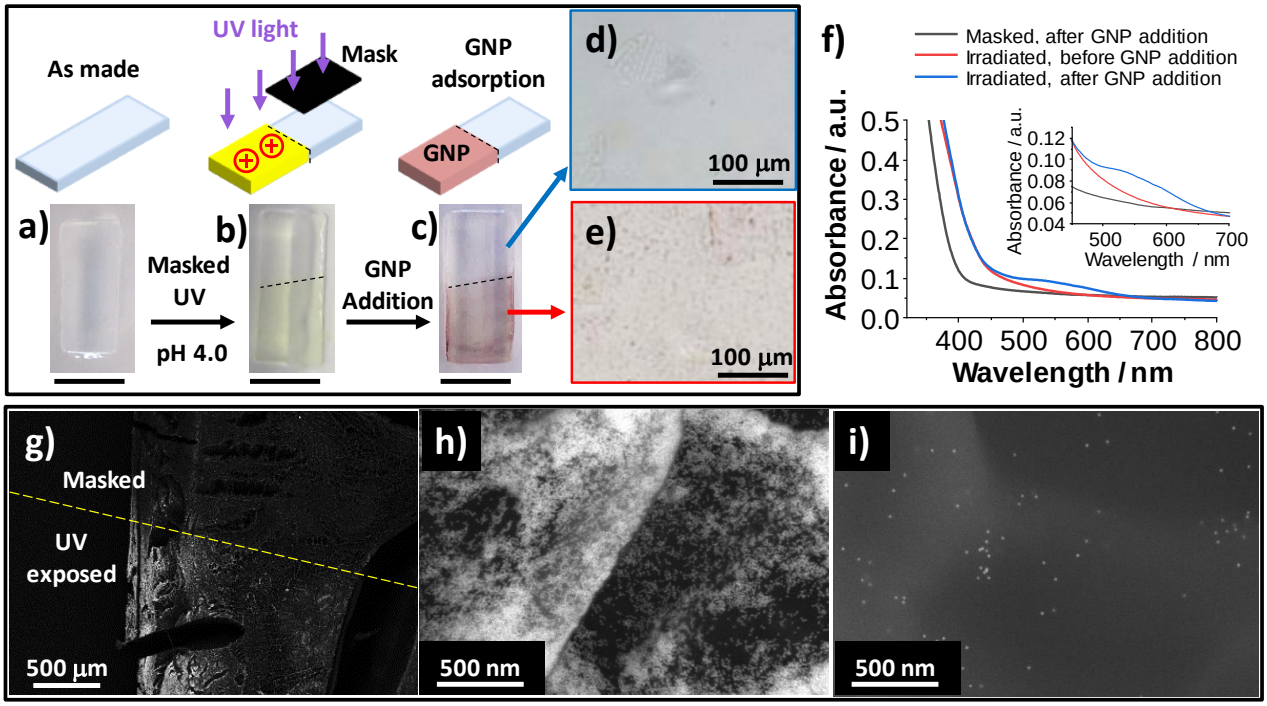

Figure 4. Spatially-selective adsorption of negatively charged GNPs onto PAAm/MBA-PBG(2) hydrogel. (a) shows the non-irradiated hydrogel, (b) is after UV-irradiation on half of the sample and adjusting the pH to 4.0. (c) shows the hydrogel after immersion into GNP dispersion. The scale bars are 4.0 mm. (d) and (e) are optical micrographs of areas with and without GNPs adsorption respectively. (f) shows UV-visible spectra for the UV-irradiated area before and after addition of GNPs and also the masked area after addition of GNP. (g - i) are SEM images of freeze-dried sample shown in (c). (g) shows the sample at lower magnification where the boundary of UV-irradiated and masked area can be observed. (h) and (i) were taken at higher magnification focused on the UV-irradiated area with copious number of GNPs (h) and the masked area with fewer GNPs (i).

Figure 4d and 4e are light microscope images and indicate regions of aggregated GNPs on the surface of the UV-irradiated area; whereas, on the photomasked area there were no evidence of GNPs. UV-visible spectroscopy measurements (Figure 4f) confirmed GNP adsorption and supported the light microscope images. The spectra were obtained from different areas of the same sample. Initially a UV-visible spectrum of a UV-irradiated area was obtained. Then the sample was soaked in a GNP dispersion followed by washing with water. After GNP deposition the UV-visible spectrum of both the UV-irradiated and masked area was measured. A broad peak, which was related to surface plasmon resonance (SPR) of GNPs, was observed only for the region subjected to UV-irradiation. The broad SPR peak was result of GNPs aggregation[49] when compared to UV-vis spectra of pure

GNP dispersion (see Figure S16). The λ_{max} of SPR peak for the latter was 520 nm and it shifted to 551 nm for the adsorbed GNPs.

The adsorption of GNPs onto PAAm/MBA-PBG(2) hydrogel was further investigated using SEM. Figure 4g - 4i show SEM images that were obtained with a backscattered detector. There was a dramatic difference in the number of GNPs in the UV-irradiated area compared to the masked area. Elemental mapping was also performed using energy-dispersive X-ray detector and showed a stronger gold signal for the UV-irradiated area (Figure S17).

3.5 Spatially controlled polymerization within the pre-formed hydrogel network

The ability of PBG nanoparticles to switch the local negative charge to positive on demand also enabled space-selective post-polymerization within the PAAm hydrogel network. This process is particularly notable when spatiotemporal post-modification of chemical and physical properties of hydrogels is needed.[50-51] We show that it was possible to absorb anionic initiator such as APS into a UV-irradiated area which possessed positive charge. Figures 5a - 5c depict PAAm/MBA-PBG(4) hydrogel film which one half was UV-irradiated. The anionic persulfate groups were absorbed into the gel at pH 2.0 into both photo-masked and UV-irradiated area, but only the latter retained the persulfate ions after washing step due to electrostatic attraction. When the sample was immersed in 2-hydroxyethyl methacrylate (HEMA) monomer and crosslinker (MBA), a PHEMA network formed upon heating. To let the sample swell and remove the unreacted monomers, it was then left in water at 50 °C. The UV-irradiated area shrunk during the polymerization (Figure 5c) due to formation of the PHEMA network which is less hydrophilic compared to PAAm[52]. After reaching swelling equilibrium in water at elevated temperature, the UV-irradiated region was ~ 3.5 times less swollen compared to the volume of the masked area.

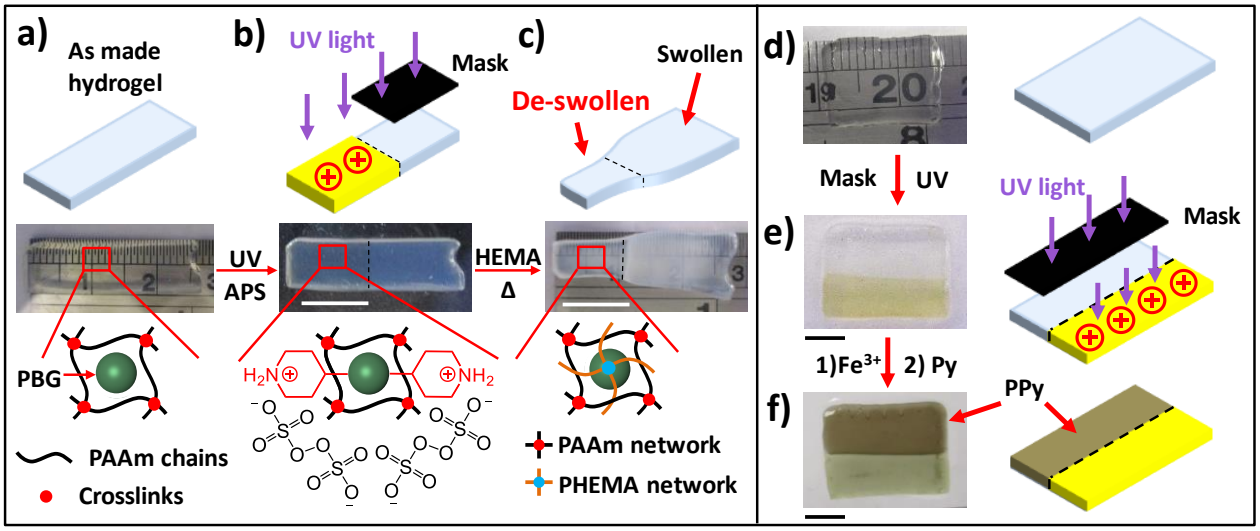

Figure 5. Space-selective positive fabrication of poly(HEMA/MBA) within PAAm/MBA-PBG(4) hydrogel on the UV-irradiated side (a-c). (a) is the as made PAAm/MBA-PBG(4) sample. (b) is after UV-irradiation on half of the sample and addition of APS. The persulfate anions were absorbed selectively to the UV-irradiated half. Formation of a PHEMA network (depicted in cartoon) minimizes swelling of hydrogel in the UV-irradiated area, shown in (c). The scale bars in (b) and (c) are 1 cm. Space-selective negative fabrication of polypyrrole in PAAm/MBA-PBG(4) at the masked area is shown in (d-f). (d) is the as made sample (e) is after UV-irradiation on half of sample. (f) shows the sample after polymerization of pyrrole. The scale bar in (e) and (f) indicates 5 mm.

Spatial control over electrical conductivity is a prerequisite for developing hydrogel based electronics such as electronic skin.[53] We therefore absorbed cations (Fe^{3+}) within the photo-masked area, which possessed a net negative charge, to alter the electrical conductivity by post-polymerization of pyrrole. This process is negative fabrication process when compared to the PHEMA network growth discussed above. Figure 5d illustrates an as-made PAAm/MBA-PBG(4) hydrogel film. One half of sample was UV-irradiated and left in pH 2.0 medium to generate positive charge to repel mobile cations (Figure 5e). The sample was then placed in $FeCl_3$ solution to enable Fe^{3+} cations to absorb within the negatively charged sites in the non-UV-irradiated half. After a washing step with dilute HCl to remove non-absorbed Fe^{3+} ions the sample was soaked in pyrrole solution and the color of the photo-masked area turned black indicating oxidative polymerization of pyrrole (Figure 5f).[54] Formation of polypyrrole was confirmed by UV-visible spectroscopy (see Figure S18) as a peak appeared at 460 nm related π to π^* transition of polypyrrole.[55] The electrical conductivity values of masked and UV-

irradiated area, were measured as 3.1×10^{-3} S/cm and 2.9×10^{-4} S/cm respectively. This indicates an increase of more than 10 fold in the electrical conductivity due to space-selective formation of polypyrrole in the masked area. The slight electrical conductivity in UV-irradiated side can largely be attributed to the presence of residual ions. However, we cannot rule out a contribution from a small amount of polypyrrole that may have formed due to binding of Fe^{3+} ions to negative charge from the initiator residues. A light emitting diode (LED) circuit was also used to visualize the difference in electrical conductivity of UV-irradiated and masked area after post-polymerization of pyrrole (see Figure S19 and Movie S1).

3.6 Photogradient generated actuator and gripper

Hydrogel actuators are mostly fabricated in a bilayer design which makes them tedious to prepare as often several complicated steps are required.[56-58] We designed a monolayer actuator and gripper by employing both PAG and PBG nanoparticles. When a 1:1 mixture of PAG and PBG were embedded into PAAm hydrogel, it was possible to increase the concentration of both negative and positive charges simultaneously by UV-irradiation. The electrostatic attraction forces between UV-irradiated PAG and PBG nanoparticles led to pH-dependent deswelling of the PAAm hydrogel network. To demonstrate this effect rheological data were obtained for PAAm/MBA-PAG(1)/PBG(1) hydrogel. The concentrations of both parent PAG and PBG dispersions were 1.0 wt%. The frequency-sweep data indicated that the storage modulus (*G'*) value increased by a factor of ~ 3 from 160 Pa to 435 Pa after UV-irradiation (Figure S20a). The increase in the *G'* value and the consequent deswelling (see Figure S20b Inset) is due to colloidal-scale particle-to-particle crosslinking between anionic PAG and cationic PBG nanoparticles after UV-irradiation. The latter did not significantly affect the ductility of the PAAm/MBA-PAG(1)/PBG(1) hydrogel as can be concluded from strain-sweep data shown in Figure S20b. The critical strain value (i.e. strain where *G' = G"*) was ~ 130 % for both the control and the UV-irradiated sample. The fact that the latter values are the same implies that PAAm/MBA-PAG(1)/PBG(1) gel breakdown is governed by the PAAm/MBA network.

The average separation between the particle centers (L) for PAAm/MBA-PAG(1)/PBG(1) can be estimated using the relationship, $L = N_p^{-1/3}$, where N_p is number-density of particles[59]. This equation assumes the particles are dispersed as a non-close-packed cubic lattice. Using an average particle diameter of 20 nm and a density of 1 g/cm^3 the calculated L value is 60 nm and the separation between surfaces is 40 nm. The experimental observations of a light-triggered modulus increase (Figure S20) strongly suggest that the particles were much more closely spaced than estimated from this simple model. We suggest that during the formation of PAAm/MBA-PAG(1)/PBG(1) gel some of the PAG and PBG particles are pushed closer together as a result of PAAm/MBA network growth. These closely situated particles form particle-particle bonds after UV-irradiation.

We posited that for lower concentrations of nanoparticles (< 5.0 wt%) UV light can pass through the sample and reach the lower layers of the hydrogel, however, for higher total concentrations (> 5.0 wt%), due to pronounced light scattering, the UV light (e.g. 300 nm), can only interact with the nanoparticles close to the surface. (An assessment of light penetration within the gels is given in the Supporting Information.) This idea enabled us to prepare PAAm/MBA-PAG(3)/PBG(3) hydrogel actuators that were fabricated in one layer. This contrasts with conventional actuators prepared using multiple layers.[56-58] Figure 6a show PAAm/MBA-PAG(3)/PBG(3) hydrogel film which was prepared from 3.0 wt% parent PAG/PBG dispersion. Only one half of the hydrogel film was irradiated by UV light.

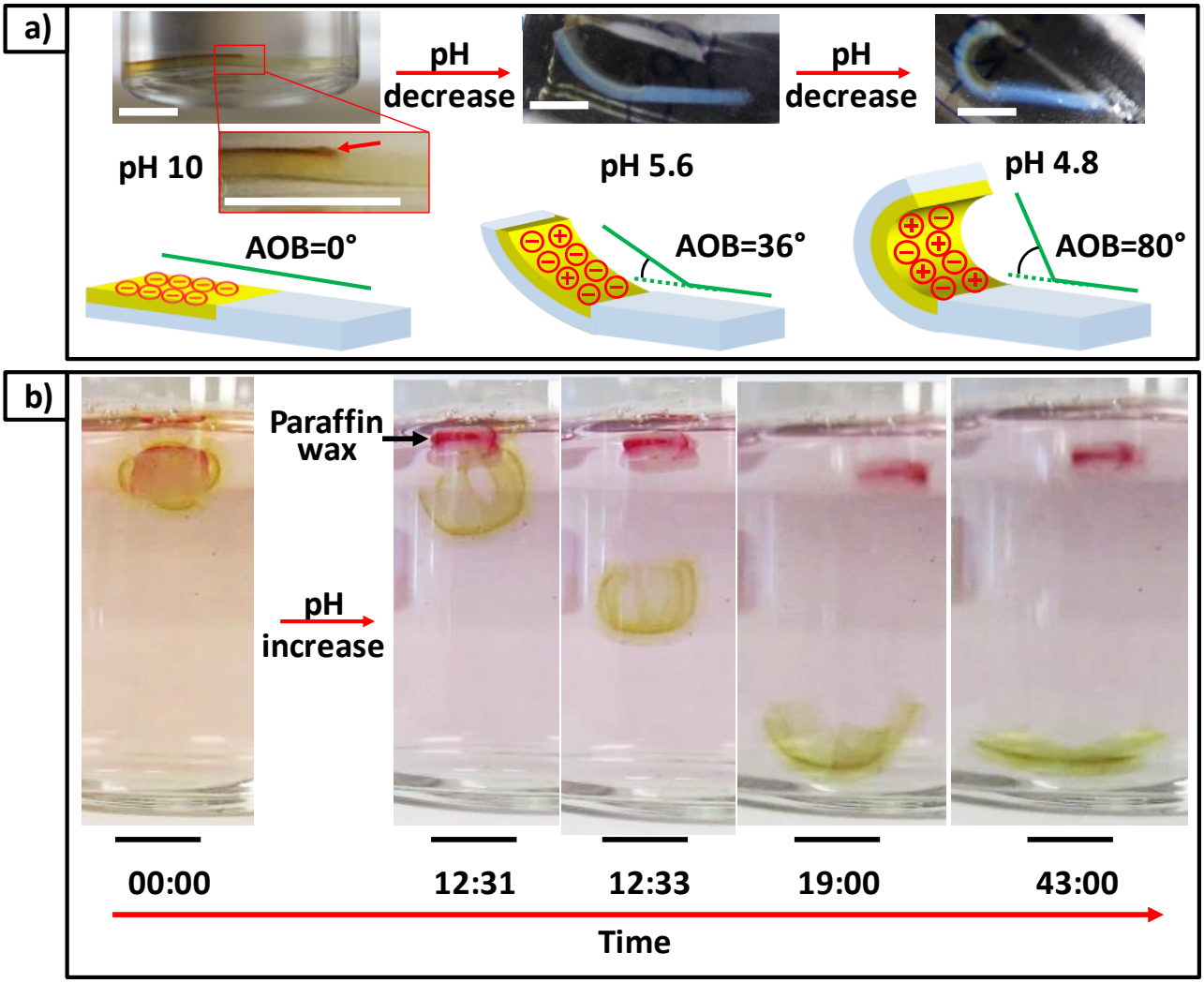

Figure 6. (a) shows a monolayer actuator that responds to pH alteration. The actuator was composed of PAAm/MBA-PAG(3)/PBG(3). Only one half of hydrogel film was UV-irradiated (from the top). The cartoon shows the top view. The maximum actuation effect was observed at pH 4.8. The scale bars show 5 mm. (b) shows a gripper with same composition as the actuator and it grabs a low density object (paraffin stained pink). The initial pH (time 00:00 mm:ss) was 4.8 as the universal pH indicator was orange. The pH was increased to 10 by addition of NaOH 0.1 M which caused the color of the pH indicator to turn pink. At time 12:31 the gripper released the object and sank to bottom of beaker. The arms were fully open after a time of 43 min. The scale bars are 1 cm.

The area close to the surface subjected to UV light deswelled when the pH was decreased. The depth of UV penetration was approximately 130 μm from the surface as determined from the color change, because of photo-chemical reaction, which can be seen from the expanded cross-section view in Figure 6a. The angle of bending (AOB) was pH-dependent and by lowering the pH its value increased from 0° at pH 10 to 80° at pH 4.8. Other monolayer photo-responsive hydrogel actuators were

reported earlier based on anthracene chemistry but these systems reached a small AOB which might restrict their use in devices such as grippers[60].

Recently hydrogel grippers have attracted significant interest in the field of soft robotics.[3] The actuation effect with a large AOB enabled us to fabricate a hydrogel gripper using the LTPHP approach. The cross-shape gripper with weight of 0.25 g had four arms which were UV-irradiated from top. Figure 6b shows that at acidic pH (universal pH indicator is orange) the gripper arms are closed whilst grabbing a floating object (a piece of paraffin wax) causing the gripper (and wax) to float in pH 4.8 water. By increasing the pH to 10 (universal pH indicator is pink) the gripper arms started to open due to amine de-protonation which decreased electrostatic attraction between PAG and PBG nanoparticles. Consequently, the gripper sank to the bottom of beaker. The arms were fully opened over time when gripper equilibrated in alkaline water. The whole process is shown in Movie S2. Hence, the incorporation of a mixture of PAG and PBG nanoparticles into a non-ionic hydrogel transformed it to a monolayer pH-triggered gripper by utilizing light scattering as a benefit which is unique to colloidal systems. If required, one way to increase the strength of these new grippers in future would be to increase the concentration of light-triggered particle-to-particle crosslinks. A second method would be to increase the AAm and / or MBA concentrations used during PAAm hydrogel synthesis.

4. Conclusions

We have showcased a versatile new approach (LTPHP) that introduces various functionalities at targeted area of non-ionic hydrogels by altering the electrostatic charge density and polarity of hydrogels. We designed and synthesized transparent sub-50 nm PAG / PBG generator nanoparticles and embedded them into PAAm hydrogel. The PAG nanoparticles were capable of producing negative charges at alkaline pHs and resulted in photo triggered swelling of hydrogels. The value of swelling ratio was 40 at pH 4.0 and reached 100 at pH 9.2 for UV-irradiated PAAm hydrogel. Using PBG nanoparticles, which were a source of positive charges, we were able to space-selectively absorb

ions into the hydrogel; therefore writing and erasing patterns reversibly was possible by utilizing ionic dyes. Negatively charged nanoparticles such as GNP were also adsorbed space-selectively onto surface of PAAm hydrogels containing PBG nanoparticles. Space-selective post-polymerization of HEMA as well as pyrrole in pre-formed PAAm was achieved by incorporating PBG nanoparticles. The PAG/PBG nanoparticles caused deswelling of the macroscopic PAAm hydrogel due to physical crosslinking between PAG and PBG nanoparticles. Additionally we showed that by adjusting the concentration of PAG/PBG nanoparticles we could control light penetration into the hydrogel, enabling construction of monolayer actuator and gripper with large angle of bending without having to use bilayers. We envisage that our LTPHP approach may open new ways for fabricating novel functional materials with numerous potential applications such as soft actuators/grippers, electronic skin and adaptive surfaces.

Supporting Information

The Supporting Information is available free of charge at https://pubs.acs.org

Additional experimental details, tables showing characterization data for the particles and compositions for the hydrogels, depiction of the UV-irradiation geometry, ^{1}H NMR spectra for DMNBM and PAG and PBG, UV-visible spectra for PAG and PBG particles, selected gels, GNP-coated gels and gels containing polypyrrole, potentiometric titration data for the PAG particles, volume swelling ratio for the PAG particles, TEM size distributions for the particles, SEM of PAAm/MBA-PAG(4) gel and gels containing adsorbed GNPs, swelling data for the gels containing adsorbed GNPs, TEM for the GNPS, photographs of circuit used to show conductivity of gels containing polypyrrole, rheology data, assessment of light penetration within the gels (PDF).

Two movies are included: Illustration of electrical conductivity in two different regions of PAAm/MBA-PBG(4) hydrogel film and the gripper response to pH.

Acknowledgements

This work was supported by a 5-year EPSRC Established Career Fellowship awarded to B.R.S. (EP/M002020/1). The authors wish to thank the staff in the FBMH EM Core Facility for their assistance and the Wellcome Trust for equipment grant support to the EM Facility.

References

1. Mitragotri, S.; Burke, P. A.; Langer, R., Overcoming the challenges in administering biopharmaceuticals: formulation and delivery strategies. *Nat. Rev. Drug Discovery* **2014,** *13*, 655-672.

2. Pi, Q.; Maharjan, S.; Yan, X.; Liu, X.; Singh, B.; van Genderen, A. M.; Robledo-Padilla, F.; Parra-Saldivar, R.; Hu, N.; Jia, W.; Xu, C.; Kang, J.; Hassan, S.; Cheng, H.; Hou, X.; Khademhosseini, A.; Zhang, Y. S., Digitally Tunable Microfluidic Bioprinting of Multilayered Cannular Tissues. *Adv. Mater.* **2018,** *30*, 1706913.

3. Yuk, H.; Lin, S.; Ma, C.; Takaffoli, M.; Fang, N. X.; Zhao, X., Hydraulic hydrogel actuators and robots optically and sonically camouflaged in water. *Nat. Commun.* **2017,** *8*, 14230.

4. Palleau, E.; Morales, D.; Dickey, M. D.; Velev, O. D., Reversible patterning and actuation of hydrogels by electrically assisted ionoprinting. *Nat. Commun.* **2013,** *4*, 2257.

5. Cheng, E.; Xing, Y.; Chen, P.; Yang, Y.; Sun, Y.; Zhou, D.; Xu, L.; Fan, Q.; Liu, D., A pH-Triggered, Fast-Responding DNA Hydrogel. *Angew. Chem. Int. Ed.* **2009,** *48*, 7660-7663.

6. Qin, H.; Zhang, T.; Li, N.; Cong, H.-P.; Yu, S.-H., Anisotropic and self-healing hydrogels with multi-responsive actuating capability. *Nat. Commun.* **2019,** *10*, 2202.

7. Ming, Z.; Ruan, X.; Bao, C.; Lin, Q.; Yang, Y.; Zhu, L., Micropatterned Protein for Cell Adhesion through Phototriggered Charge Change in a Polyvinylpyrrolidone Hydrogel. *Adv. Funct. Mater.* **2017,** *27*, 1606258.

8. Ercole, F.; Davis, T. P.; Evans, R. A., Photo-responsive systems and biomaterials: photochromic polymers, light-triggered self-assembly, surface modification, fluorescence modulation and beyond. *Polym. Chem.* **2010,** *1*, 37-54.

9. Luo, Y.; Shoichet, M. S., A photolabile hydrogel for guided three-dimensional cell growth and migration. *Nat. Mater.* **2004,** *3*, 249-253.

10. Zuo, B.; Wang, M.; Lin, B.-P.; Yang, H., Photomodulated Tricolor-Changing Artificial Flowers. *Chem. Mater.* **2018,** *30*, 8079-8088.

11. Guo, H.; Uehara, Y.; Matsuda, T.; Kiyama, R.; Li, L.; Ahmed, J.; Katsuyama, Y.; Nonoyama, T.; Kurokawa, T., Surface charge dominated protein absorption on hydrogels. *Soft Matter* **2020,** *16*, 1897-1907.

12. Li, D.; Zhang, X.; Yao, J.; Simon, G. P.; Wang, H., Stimuli-responsive polymer hydrogels as a new class of draw agent for forward osmosis desalination. *Chem. Commun.* **2011,** *47*, 1710-1712.

13. Fu, F.; Chen, Z.; Wang, H.; Liu, C.; Liu, Y.; Zhao, Y., Graphene hybrid colloidal crystal arrays with photo-controllable structural colors. *Nanoscale* **2019,** *11*, 10846-10851.

14. Kelly, J. A.; Shukaliak, A. M.; Cheung, C. C. Y.; Shopsowitz, K. E.; Hamad, W. Y.; MacLachlan, M. J., Responsive Photonic Hydrogels Based on Nanocrystalline Cellulose. *Angew. Chem. Int. Ed.* **2013,** *52*, 8912-8916.

15. Liu, J.; Xie, C.; Kretzschmann, A.; Koynov, K.; Butt, H.-J.; Wu, S., Metallopolymer Organohydrogels with Photo-Controlled Coordination Crosslinks Work Properly Below 0 °C. *Adv. Mater.* **2020,** *32*, 1908324.

16. Luo, R.-C.; Lim, Z. H.; Li, W.; Shi, P.; Chen, C.-H., Near-infrared light triggerable deformation-free polysaccharide double network hydrogels. *Chem. Commun.* **2014,** *50*, 7052-7055.

17. Lv, S.-W.; Liu, Y.; Xie, M.; Wang, J.; Yan, X.-W.; Li, Z.; Dong, W.-G.; Huang, W.-H., Near-Infrared Light-Responsive Hydrogel for Specific Recognition and Photothermal Site-Release of Circulating Tumor Cells. *ACS Nano* **2016,** *10*, 6201-6210.

18. Yoshii, T.; Ikeda, M.; Hamachi, I., Two-Photon-Responsive Supramolecular Hydrogel for Controlling Materials Motion in Micrometer Space. *Angew. Chem. Int. Ed.* **2014,** *53*, 7264-7267.

19. Zhang, X.; Pint, C. L.; Lee, M. H.; Schubert, B. E.; Jamshidi, A.; Takei, K.; Ko, H.; Gillies, A.; Bardhan, R.; Urban, J. J.; Wu, M.; Fearing, R.; Javey, A., Optically- and Thermally-Responsive

Programmable Materials Based on Carbon Nanotube-Hydrogel Polymer Composites. *Nano Lett.* **2011,** *11*, 3239-3244.

20. Iwaso, K.; Takashima, Y.; Harada, A., Fast response dry-type artificial molecular muscles with [c2]daisy chains. *Nat. Chem.* **2016,** *8*, 625-632.

21. Tsang, K. M. C.; Annabi, N.; Ercole, F.; Zhou, K.; Karst, D. J.; Li, F.; Haynes, J. M.; Evans, R. A.; Thissen, H.; Khademhosseini, A.; Forsythe, J. S., Facile One-Step Micropatterning Using Photodegradable Gelatin Hydrogels for Improved Cardiomyocyte Organization and Alignment. *Adv. Funct. Mater.* **2015,** *25*, 977-986.

22. Qiu, Z.; Yu, H.; Li, J.; Wang, Y.; Zhang, Y., Spiropyran-linked dipeptide forms supramolecular hydrogel with dual responses to light and to ligand–receptor interaction. *Chem. Commun.* **2009**, 3342-3344.

23. Zhao, Y.-L.; Stoddart, J. F., Azobenzene-Based Light-Responsive Hydrogel System. *Langmuir* **2009,** *25*, 8442-8446.

24. Peng, K.; Tomatsu, I.; Kros, A., Light controlled protein release from a supramolecular hydrogel. *Chem. Commun.* **2010,** *46*, 4094-4096.

25. Tamesue, S.; Takashima, Y.; Yamaguchi, H.; Shinkai, S.; Harada, A., Photoswitchable Supramolecular Hydrogels Formed by Cyclodextrins and Azobenzene Polymers. *Angew. Chem. Int. Ed.* **2010,** *49*, 7461-7464.

26. Valdes, L. B., Resistivity Measurements on Germanium for Transistors. *Proc. IRE* **1954,** *42*, 420-427.

27. Gaplovsky, M.; Il'ichev, Y. V.; Kamdzhilov, Y.; Kombarova, S. V.; Mac, M.; Schwörer, M. A.; Wirz, J., Photochemical reaction mechanisms of 2-nitrobenzyl compounds: 2-Nitrobenzyl alcohols form 2-nitroso hydrates by dual proton transfer. *Photochem. Photobiol. Sci.* **2005,** *4*, 33-42.

28. Herman, B.; Lemasters, J. J., *Optical Microscopy: Emerging Methods and Applications*. Elsevier Science: 2012.

29. Milani, A. H.; Saunders, J. M.; Nguyen, N. T.; Ratcliffe, L. P. D.; Adlam, D. J.; Freemont, A. J.; Hoyland, J. A.; Armes, S. P.; Saunders, B. R., Synthesis of polyacid nanogels: pH-responsive sub-100 nm particles for functionalisation and fluorescent hydrogel assembly. *Soft Matter* **2017,** *13*, 1554-1560.

30. Das, M.; Mardyani, S.; Chan, W. C. W.; Kumacheva, E., Biofunctionalized pH-Responsive Microgels for Cancer Cell Targeting: Rational Design. *Adv. Mater.* **2006,** *18*, 80-83.

31. Dalmont, H.; Pinprayoon, O.; Saunders, B. R., Study of pH-Responsive Microgels Containing Methacrylic Acid: Effects of Particle Composition and Added Calcium. *Langmuir* **2008,** *24*, 2834-2840.

32. P. Hay, M.; M. Sykes, B.; A. Denny, W.; J. O'Connor, C., Substituent effects on the kinetics of reductively-initiated fragmentation of nitrobenzyl carbamates designed as triggers for bioreductive prodrugs. *J. Chem. Soc., Perkin Trans. 1* **1999**, 2759-2770.

33. Amalvy, J. I.; Wanless, E. J.; Li, Y.; Michailidou, V.; Armes, S. P.; Duccini, Y., Synthesis and Characterization of Novel pH-Responsive Microgels Based on Tertiary Amine Methacrylates. *Langmuir* **2004,** *20*, 8992-8999.

34. Hu, L.; Chu, L.-Y.; Yang, M.; Wang, H.-D.; Hui Niu, C., Preparation and characterization of novel cationic pH-responsive poly(N,N′-dimethylamino ethyl methacrylate) microgels. *J. Coll. Interf. Sci.* **2007,** *311*, 110-117.

35. Phelps, E. A.; Enemchukwu, N. O.; Fiore, V. F.; Sy, J. C.; Murthy, N.; Sulchek, T. A.; Barker, T. H.; García, A. J., Maleimide Cross-Linked Bioactive PEG Hydrogel Exhibits Improved Reaction Kinetics and Cross-Linking for Cell Encapsulation and In Situ Delivery. *Adv. Mater.* **2012,** *24*, 64-70.

36. Duncombe, T. A.; Kang, C.-C.; Maity, S.; Ward, T. M.; Pegram, M. D.; Murthy, N.; Herr, A. E., Hydrogel Pore-Size Modulation for Enhanced Single-Cell Western Blotting. *Adv. Mater.* **2016,** *28*, 327-334.

37. Yetisen, A. K.; Jiang, N.; Fallahi, A.; Montelongo, Y.; Ruiz-Esparza, G. U.; Tamayol, A.; Zhang, Y. S.; Mahmood, I.; Yang, S.-A.; Kim, K. S.; Butt, H.; Khademhosseini, A.; Yun, S.-H., Glucose-Sensitive Hydrogel Optical Fibers Functionalized with Phenylboronic Acid. *Adv. Mater.* **2017,** *29*, 1606380.

38. Tutar, R.; Motealleh, A.; Khademhosseini, A.; Kehr, N. S., Functional Nanomaterials on 2D Surfaces and in 3D Nanocomposite Hydrogels for Biomedical Applications. *Adv. Funct. Mater.* **2019,** *29*, 1904344.

39. Zhan, H.; Löwik, D. W. P. M., A Hybrid Peptide Amphiphile Fiber PEG Hydrogel Matrix for 3D Cell Culture. *Adv. Funct. Mater.* **2019,** *29*, 1808505.

40. Klinger, D.; Landfester, K., Photo-sensitive PMMA microgels: light-triggered swelling and degradation. *Soft Matter* **2011,** *7*, 1426-1440.

41. Xie, F.; Qin, L.; Liu, M., A dual thermal and photo-switchable shrinking–swelling supramolecular peptide dendron gel. *Chem. Commun.* **2016,** *52*, 930-933.

42. Krsko, P.; Kaplan, J. B.; Libera, M., Spatially controlled bacterial adhesion using surface-patterned poly(ethylene glycol) hydrogels. *Acta Biomater.* **2009,** *5*, 589-596.

43. Galindo, F.; Lima, J. C.; Luis, S. V.; Parola, A. J.; Pina, F., Write–Read–Erase Molecular-Switching System Trapped in a Polymer Hydrogel Matrix. *Adv. Funct. Mater.* **2005,** *15*, 541-545.

44. Yang, Y.; Guan, L.; Gao, G., Low-Cost, Rapidly Responsive, Controllable, and Reversible Photochromic Hydrogel for Display and Storage. *ACS Appl. Mater. Interf.* **2018,** *10*, 13975-13984.

45. Xiao, S.; Paukstelis, P. J.; Ash, R. D.; Zavalij, P. Y.; Davis, J. T., Drawing with Iron on a Gel Containing a Supramolecular Siderophore. *Angew. Chem. Int. Ed.* **2019,** *58*, 18434-18437.

46. Piras, C. C.; Smith, D. K., Sequential Assembly of Mutually Interactive Supramolecular Hydrogels and Fabrication of Multi-Domain Materials. *Chem. - Eur. J.* **2019,** *25*, 11318-11326.

47. Ren, F.; Yesildag, C.; Zhang, Z.; Lensen, M. C., Functional PEG-Hydrogels Convey Gold Nanoparticles from Silicon and Aid Cell Adhesion onto the Nanocomposites. *Chem. Mater.* **2017,** *29*, 2008-2015.

48. Wu, S.; Zhu, M.; Lian, Q.; Lu, D.; Spencer, B.; Adlam, D. J.; Hoyland, J. A.; Volk, K.; Karg, M.; Saunders, B. R., Plasmonic and colloidal stability behaviours of Au-acrylic core–shell nanoparticles with thin pH-responsive shells. *Nanoscale* **2018,** *10*, 18565-18575.

49. Carnerero, J. M.; Jimenez-Ruiz, A.; Grueso, E. M.; Prado-Gotor, R., Understanding and improving aggregated gold nanoparticle/dsDNA interactions by molecular spectroscopy and deconvolution methods. *Phys. Chem. Chem. Phys.* **2017,** *19*, 16113-16123.

50. Jungnickel, C.; Tsurkan, M. V.; Wogan, K.; Werner, C.; Schlierf, M., Bottom-Up Structuring and Site-Selective Modification of Hydrogels Using a Two-Photon [2+2] Cycloaddition of Maleimide. *Adv. Mater.* **2017,** *29*, 1603327.

51. De France, K. J.; Hoare, T.; Cranston, E. D., Review of Hydrogels and Aerogels Containing Nanocellulose. *Chem. Mater.* **2017,** *29*, 4609-4631.

52. Lakes, R. S.; Park, J. B., *Biomaterials: An Introduction*. Springer US: 2012.

53. Lin, S.; Yuk, H.; Zhang, T.; Parada, G. A.; Koo, H.; Yu, C.; Zhao, X., Stretchable Hydrogel Electronics and Devices. *Adv. Mater.* **2016,** *28*, 4497-4505.

54. Lee, J. M.; Lee, D. G.; Lee, S. J.; Kim, J. H.; Cheong, I. W., One-Step Synthetic Route for Conducting Core−Shell Poly(styrene/pyrrole) Nanoparticles. *Macromolecules* **2009,** *42*, 4511-4519.

55. Turkevich, J.; Stevenson, P. C.; Hillier, J., A study of the nucleation and growth processes in the synthesis of colloidal gold. *Discuss. Faraday Soc.* **1951,** *11*, 55-75.

56. Lu, D.; Zhu, M.; Wu, S.; Lian, Q.; Wang, W.; Adlam, D.; Hoyland, J. A.; Saunders, B. R., Programmed Multiresponsive Hydrogel Assemblies with Light-Tunable Mechanical Properties, Actuation, and Fluorescence. *Adv. Funct. Mater.* **2020,** *30*, 1909359.

57. Wei, S.; Lu, W.; Le, X.; Ma, C.; Lin, H.; Wu, B.; Zhang, J.; Theato, P.; Chen, T., Bioinspired Synergistic Fluorescence-Color-Switchable Polymeric Hydrogel Actuators. *Angew. Chem. Int. Ed.* **2019,** *58*, 16243-16251.

58. Stoychev, G.; Guiducci, L.; Turcaud, S.; Dunlop, J. W. C.; Ionov, L., Hole-Programmed Superfast Multistep Folding of Hydrogel Bilayers. *Adv. Funct. Mater.* **2016,** *26*, 7733-7739.

59. Kryuchkov, Y. N., Concentration Dependence of the Mean Interparticle Distance in Disperse Systems. *Refract. Ind. Ceram.* **2001,** *42*, 390-392.

60. Jiang, Z.; Tan, M. L.; Taheri, M.; Yan, Q.; Tsuzuki, T.; Gardiner, M. G.; Diggle, B.; Connal, L. A., Strong, Self-Healable, and Recyclable Visible-Light-Responsive Hydrogel Actuators. *Angew. Chem. Int. Ed.* **2020,** *59*, 7049-7056.

Table of contents